

Article

Study on the Milling Machinability of Bamboo-Based Fiber Composites

Yucheng Ding^{1,2}, Tongbin Liu^{1,3,*}, Yaqiang Ma^{1,3}, Chunmei Yang^{1,3}, Changyu Shi^{1,3}, Yongjian Cao⁴
and Jiawei Zhang^{2,*}

¹ Forestry and Woodworking Machinery Engineering Technology Center, Northeast Forestry University, Harbin 150040, China; dingyucheng@nefu.edu.cn (Y.D.); myqhit@nefu.edu.cn (Y.M.); ycmnefu@nefu.edu.cn (C.Y.); 2021115848@nefu.edu.cn (C.S.)

² Supervision and Inspection Center, Harbin 150006, China

³ College of Mechanical and Electrical Engineering, Northeast Forestry University, Harbin 150040, China

⁴ Guangdong Academy of Forestry, Guangdong 510520, China; yjcao@sinogaf.cn

* Correspondence: ltb1161879674@nefu.edu.cn (T.L.); zjw@nefu.edu.cn (J.Z.)

Abstract: Bamboo-based fiber composites, known as recombinant bamboo, have emerged as a new material in the construction and decoration industry. With its excellent mechanical and ornamental properties, recombinant bamboo is gaining popularity. However, its high hardness and abrasion resistance pose challenges in the milling process. To address this, we conducted an experimental study to investigate the milling machinability of recombinant bamboo. We studied the impact of various factors—fiber angle, feed rate, and spindle speed—on the tangential and normal roughness of milled surfaces. Our findings indicated that increasing the spindle speed within an acceptable range can effectively mitigate issues such as carbonization and endface cracking on a milled surface. Additionally, we developed a prediction model to assess the probability of end splitting in recombinant bamboo. This research aimed to enhance the milling quality of recombinant bamboo, improve control over surface roughness, reduce the likelihood of end splitting, and, ultimately, expand application possibilities.

Keywords: bamboo-based fiber composites; polymer–matrix composites; recombinant bamboo; workability; splitting inhibition; milling performance; surface roughness; milling defects



Citation: Ding, Y.; Liu, T.; Ma, Y.; Yang, C.; Shi, C.; Cao, Y.; Zhang, J. Study on the Milling Machinability of Bamboo-Based Fiber Composites.

Forests **2023**, *14*, 1924. <https://doi.org/10.3390/f14091924>

Academic Editor: Bruno Esteves

Received: 28 August 2023

Revised: 18 September 2023

Accepted: 20 September 2023

Published: 21 September 2023



Copyright: © 2023 by the authors. Licensee MDPI, Basel, Switzerland. This article is an open access article distributed under the terms and conditions of the Creative Commons Attribution (CC BY) license (<https://creativecommons.org/licenses/by/4.0/>).

1. Introduction

Bamboo possesses unique aesthetic properties and excellent mechanical properties, making it a popular choice for construction and furniture purposes [1]. Advancements in technology have led to the development of recombinant bamboo, a bamboo-based fiber composite produced via thinning, sizing, and hot-pressing processes [2,3]. Recombinant bamboo has better abrasion resistance and mechanical strength than unprocessed bamboo, while retaining its distinctive appearance [4]. This makes it ideal for applications such as landscape decoration, acoustic insulation, flooring, and outdoor furniture [5].

Machining is a crucial process for producing recombinant bamboo products, which require tongue-and-groove joints that are made possible by circumferential milling. However, the dense nature of recombinant bamboo and the uniform alignment of its fibers make efficient milling a challenging task [6,7]. Coolants cannot be used during machining, as they can negatively impact the mechanical properties of the material and increase production cycle time, thereby reducing productivity [8]. Failure to cool can lead to elevated temperatures that diminish the surface quality of processed recombinant bamboo and reduce tool lifespan [9]. Therefore, research into recombinant bamboo milling machinability is necessary to optimize milling parameters and to enhance product quality.

Previous studies by scholars have provided valuable insights into the milling properties of recombinant bamboo, forming the basis for this study. Liu et al. conducted

research on the fracture properties of recombinant bamboo and identified a three-stage fracture process: the linear stage, the softening stage, and the failure stage. The direction of bamboo fibers and the diameter of fiber bundles were found to significantly influence this process [10]. Han et al. determined the modulus of elasticity of recombinant bamboo and discovered that the ratio of shredded bamboo to bamboo fibers had a notable impact on its elasticity [11]. Costa et al. performed tensile tests on bamboo with varying fiber diameters and observed that smaller diameters resulted in higher tensile strength at the same cross-sectional area [12]. Liu et al. also investigated the impact resistance of recombinant bamboo and identified matrix, fiber-matrix interface debonding and delamination, and fiber fracture as the primary fracture forms under impact loading. They highlighted the structural form and bond strength of recombinant bamboo as the key factors influencing its impact resistance [13].

In addition to studying the machinability of recombinant bamboo milling, it was also possible in this study to refer to the machinability research of other similar carbon-fiber structures. Carbon-fiber material serves as a good example. Yang et al. [14] investigated the machinability of carbide end mills for milling carbon-fiber composites. Using optical microscopy, they assessed the milling performance based on observations of burrs and delamination on the milling surface. However, they did not provide quantitative measurements for these criteria. Chen et al. [15] developed a multi-scale framework that combined the discrete element method (DEM) and the population balance model (PBM) to evaluate and predict the machinability of alumina milling. Their evaluation metrics included particle size distribution and fineness. The accuracy of their model was also validated through experimental methods. Compared to the study by Yang et al. [14], Chen et al.'s [15] research better quantified the machinability. Wu et al. [16] investigated the cutting and machining performance of micro-end mills when grooving on 6061 aluminum. They evaluated machinability based on tool wear, surface roughness, and burr generation. Zhao et al. [17] also emphasized the importance of quantifying machinability for tool design. They used a tool as an indicator to evaluate milling performance and developed a prediction model for tool life, based on surface-roughness calculations. Yang et al. [18] employed eco-friendly pulses for carbide protection to enhance milling performance. They accurately quantified the milling force, tool wear, and surface finish quality. Additionally, they discovered a correlation between the improvement in milling performance and the magnetic field's attraction to fine chips.

Scholars' prior research has comprehensively explored the mechanical properties of recombinant bamboo and made significant advances in investigating the processing properties of metals and non-metals. In contrast, there has been relatively insufficient research on the processing characteristics of recombinant bamboo, which has hindered the quantitative processing of recombinant bamboo. Therefore, this study aims to investigate the milling machinability of recombinant bamboo, including tangential and normal roughness of the milled surface, as well as the suppression of milling defects. The research findings are expected to enhance control over the milling-surface roughness of recombinant bamboo and improve the quality of milling, ultimately increasing recombinant bamboo's application prospects.

2. Materials and Methods

2.1. Materials

The reconstituted bamboo material used in this study was sourced from Hunan Taohuajiang Bamboo Science and Technology Co. Ltd. It was derived from 2-year-old moso bamboo with a density of 750 kg/m³. The preparation process of the reconstituted bamboo can be divided into four main steps: thinning, glue impregnation, laying, and hot pressing [3,19]:

1. **Thinning:** The moso bamboo was sawed and cut into bamboo tubes with a length of 3000 mm and split longitudinally. The bamboo was then fed into a thinning machine, with the green side facing up, and passed through the machine 5 to 7 times. This

process resulted in nearly flat and fluffy bamboo panels. The bamboo panels were then dried in an air circulation oven at 85 degrees Celsius until the moisture content reached 10%.

2. Glue impregnation: The dried bamboo panels were immersed in a 15% solids phenolic resin for 6 min. Then, they were removed from the resin and hung in the air for 5 min to allow excess glue to drain off. This process continued until the mass fraction of phenolic resin reached about 13%. Finally, the panels were placed in an air circulation oven at 50 degrees Celsius to dry until the moisture content reached 12%.
3. Laying: The fully impregnated and dried bamboo panels were laid out to form 6-layer-thick slabs along the grain. This ensured proper alignment and stability during the subsequent pressing stage.
4. Hot pressing: The slabs were placed into a hot press set at 140 degrees Celsius with a thickness gauge of 25 cm. A pressure of 20 MPa was applied until the slabs were completely closed. The temperature of the core layer of the slab was then raised to 130 degrees Celsius and maintained at that level for 10 min under pressure. Then, while still in the mold, the slabs were cooled with water to 60 degrees Celsius.

Following this process, the final product of reconstituted bamboo was obtained by cutting the edges of the slab. The original size of the reconstituted bamboo was 3000 mm × 1500 mm × 25 mm. The recombined bamboo, after undergoing a series of processing steps, showed improved mechanical properties compared to those of moso bamboo. The tensile strength increased from 188.77 MPa to 354.78 MPa, and the compressive strength increased from 69.92 MPa to 129.08 MPa. The density of the recombined bamboo reached 1150 kg/m³.

To facilitate the clamping of the reconstituted bamboo in the milling machine, large bamboo pieces were cut into 50 mm × 50 mm × 25 mm pieces with different fiber directions (Figure 1), using the KH-828 cutting saw from Guangdong Shunde Mingan Machinery Manufacturing Company Limited, Guangdong City, China. Following the cutting process, the surrounding areas were sanded with sandpaper with a grit size of 100 to mitigate the influence of saw marks and ensure accurate testing.

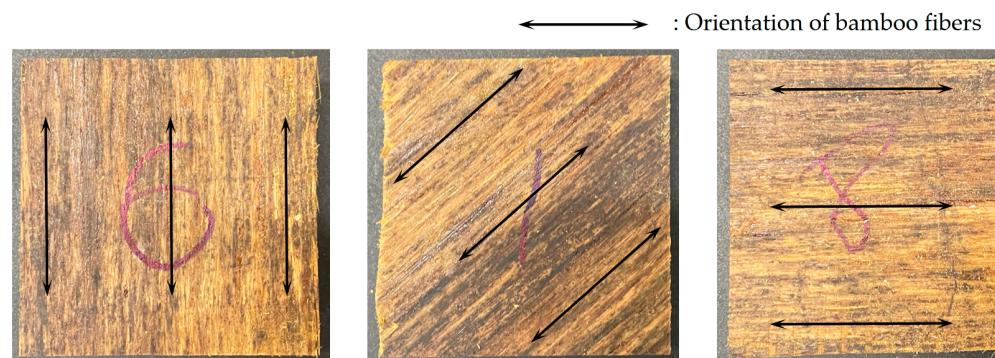


Figure 1. Recombinant bamboo with three different fiber orientations; the left side of the recombined bamboo in the figure shows the surface to be milled.

2.2. Methods

Machinability refers to the ease or difficulty that a material presents when cutting or shaping it [20]. Factors such as the material, the tensile strength, the verification rate, thermal conductivity, and impact value significantly affect machinability [21,22]. These parameters directly affect the rate of tool wear, the magnitude of the cutting force, and chip morphology. In this study, the machinability of recombined bamboo during milling was examined.

Recombined bamboo has highly directional bamboo fiber arrangement, and varying cutting directions result in different milling outcomes. Pre-tests indicated that different machining parameters had minimal impact on dimensional accuracy after machining. The

surface aesthetics and flatness of recombinant bamboo are more critical than precision, given its use as a decorative and construction material. Therefore, spindle speed and feed rate under different fiber arrangement directions were tested and evaluated using surface roughness as the primary index. It is worth noting that, in order to achieve a higher surface finish, the reorganized bamboo was processed in this study using the down milling method. Additionally, chip size and shape, as well as surface morphology, were studied under different fiber-arrangement directions.

As a result, a Box–Behnken design (BBD) test with three factors and three levels were conducted, with the factor levels presented in Table 1. The test procedure and schematic diagram of each factor are presented in Figure 2. Here, θ denotes the angle measurement between the direction of fiber arrangement and the direction of feed rate; the tangential roughness, μ_t , denotes the roughness of the milled plane parallel to the table, and the normal roughness, μ_n , denotes the roughness of the milled plane perpendicular to the table.

Table 1. Test factors and test levels.

Level	Fiber Angle θ (°)	Feed Rate v (mm/min)	Spindle Speed n (r/min)
−1	0	700	7000
0	45	1100	8500
+1	90	1500	10,000

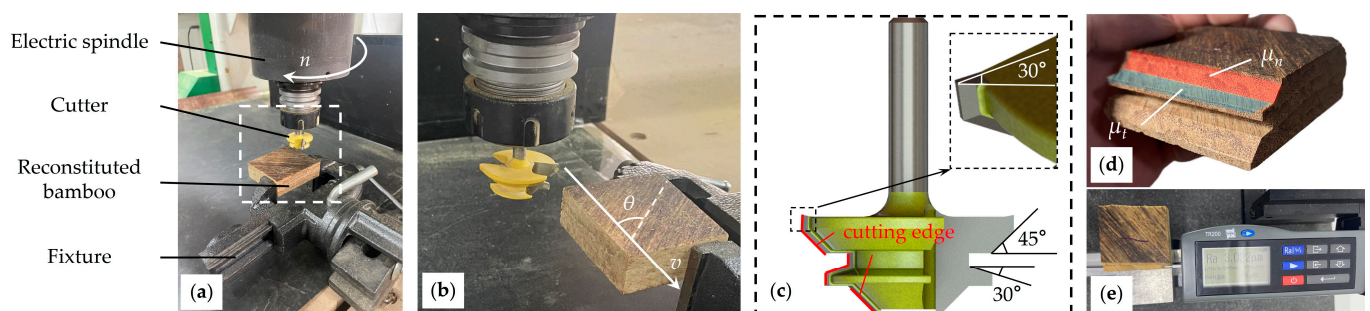


Figure 2. Procedure for milling test of recombinant bamboo. (a) Recombinant bamboo mounted on a fixture. (b) Fiber angle of recombinant bamboo. (c) Structure and angle of the milling cutter. (d) Tangential and normal roughness of the milled surface. (e) Measurement procedure of tangential roughness of milled surface.

During the study, the recombinant bamboo was clamped onto the fixture of a 3-axis machining center (MGK 06, Nanxing Equipment Company Limited, Dongguan City, China). To ensure a consistent depth of cut for each milling, special attention was given to the clamping height and of the recombinant bamboos, which was accomplished through standardized heights and depths using a gauge block. A circumferential milling cutter (model $\frac{1}{4} \times 1 - \frac{1}{2}$, Yueqing Fuxin Hardware Tool Company Limited, Wenzhou City, China) was used for all milling tasks. Each cutting edge of the milling cutter was designed with a front angle of 0° and a rear angle of 30°. Following the milling, the tangential roughness μ_t (Ra) and normal roughness μ_n (Ra) of the cutting surface were measured, using a digital surface roughness meter (TIME3220, Beijing Raguang Technology Company Limited, Beijing City, China) in accordance with the surface roughness measurement standard (GB–T12472–1990). To minimize measurement errors associated with surface roughness, three measurements were taken for each surface and averaged. To minimize the impact on roughness of varying cutting speeds resulting from different cutting radii, it was advisable to measure the tangential roughness μ_t at a location adjacent to the surface where the normal roughness μ_n was measured. This was achieved by selecting an area bordered by the blue and red regions in Figure 2c as the ideal measurement location for μ_t . Additionally, recombined bamboo chips were observed under different factors, and chip morphology changes were analyzed with alterations of the fiber angle.

3. Results and Discussion

The testing was carried out at the Forestry and Woodworking Machinery Engineering Technology Center, Northeast Forestry University, China. The temperature during the test was recorded to be 27 °C. The test results are summarized in Table 2, which includes the fiber angle θ , feed rate v , spindle speed n , average tangential roughness μ_t , and average normal roughness μ_n .

Table 2. Surface roughness measurements with different test factors.

No.	Factors			Indicators			
	θ (°)	v (mm/min)	n (r/min)	μ_t (Ra, μm)	Standard Deviation	μ_n (Ra, μm)	Standard Deviation
1	45	1100	8500	3.172	0.311	1.859	0.164
2	45	700	7000	2.897	0.273	2.147	0.272
3	45	1100	8500	3.215	0.381	1.629	0.176
4	0	1500	8500	2.495	0.164	1.64	0.139
5	45	1500	10,000	2.535	0.197	2.223	0.242
6	0	1100	7000	1.985	0.155	2.497	0.253
7	0	700	8500	1.039	0.133	0.964	0.092
8	90	1100	10,000	2.131	0.204	1.645	0.133
9	90	1500	8500	3.755	0.286	3.144	0.291
10	90	700	8500	2.113	0.167	1.748	0.215
11	90	1100	7000	2.981	0.261	2.939	0.257
12	0	1100	10,000	1.338	0.149	0.949	0.088
13	45	700	10,000	1.917	0.224	1.175	0.135
14	45	1500	7000	3.859	0.413	2.998	0.281
15	45	1100	8500	3.371	0.379	1.755	0.216

3.1. Correlation Analysis of Surface Roughness

Table 3 presents the detailed analysis of tangential roughness μ_t obtained from the research. The regression model utilized to study tangential roughness was deemed to be highly significant, as indicated by $p < 0.0001$. This finding substantiated a strong association between the factors and tangential roughness. The outcomes revealed that all three factors—fiber angle θ , feed speed v , and spindle speed n —significantly affected tangential roughness concerning $p < 0.05$. Furthermore, the squared terms of the fiber angle θ and the spindle speed n also held a remarkable level of significance, proposing a nonlinear relationship in the regression model for tangential roughness. To further explore the regression model for tangential roughness, Equation (1) was used to depict the model representation, with an R^2 value of 0.9472. Moreover, the lack-of-fit term was found to be insignificant ($p > 0.05$), indicating that the regression model was not overfitted.

Table 3. ANOVA for tangential roughness μ_t (Ra).

Source	Sum of Squares	df	Mean Square	F-Value	p-Value
Model	9.28	5	1.86	32.29	<0.0001
θ	2.12	1	2.12	36.97	0.0002
v	2.74	1	2.74	47.59	<0.0001
n	1.81	1	1.81	31.42	0.0003
θ^2	2.32	1	2.32	40.29	0.0001
n^2	0.4248	1	0.4248	7.39	0.0237
Residual	0.5173	9	0.0708	—	—
Lack of fit	0.4954	7	0.0708	6.45	0.1407
Cor total	9.80	14	—	—	—

The analysis of normal roughness μ_n is presented in Table 4, and a closer look reveals the remarkable significance of the regression model for normal roughness, with a p -value less than 0.0001. All three factors—the fiber angle θ , speed v , and spindle speed n —were

determined to exert a significant impact on normal roughness, with p -values less than 0.05. A noteworthy difference from the tangential rough model was that the effects of these factors on normal roughness were found to be linear. Equation (2) represents the regression equation for roughness, exhibiting an R^2 value of 0.8838, which indicates a high level of explanation provided by the model. Furthermore, it is worth mentioning that the lack-of-fit term showed no significant influence, as indicated by the p -value greater than 0.05. This implied that the regression model was not overfitting and provided reliable predictions for normal roughness μ_n .

$$\mu_t = -7.89146 + 0.046549\theta + 0.001462v + 0.002238n - 0.00039\theta^2 - 1.50299 \times 10^{-7}n^2 \quad (1)$$

$$\mu_n = 3.41139 + 0.009517\theta + 0.001241v - 0.000382n \quad (2)$$

Table 4. ANOVA for normal roughness μ_n (Ra).

Source	Sum of Squares	df	Mean Square	F-Value	p -Value
Model	6.07	3	2.02	27.90	<0.0001
θ	1.47	1	1.47	20.23	0.0009
v	1.97	1	1.97	27.18	0.0003
n	2.63	1	2.63	36.30	<0.0001
Residual	0.7978	11	0.0725	—	—
Lack of fit	0.7713	9	0.0857	6.46	0.1412
Cor total	6.87	14	—	—	—

The plot in Figure 3 demonstrates the correlation between tangential roughness μ_t and the factors. Specifically, the graphical data depicts that the tangential roughness increased and then decreased as the fiber clamp angle was increased. The fiber clamp angle for the highest point was approximately 60° , wherein a smaller fiber angle resulted in lower tangential roughness. However, when the fiber angle was 60° , tangential roughness started decreasing. The optimal fiber clamp angle for maximizing tangential roughness in recombinant bamboo is dependent on the feed direction and spindle rotation direction (this experiment utilized the downstream milling method). Additionally, the tangential roughness increased linearly with a rise in the feed rate, consistent with the alterations of roughness when cutting wood. Furthermore, the tangential roughness declined non-linearly with a higher spindle speed; this reduction accelerated with increasing speed. This reduction trend was basically similar to the roughness changes observed when milling wood.

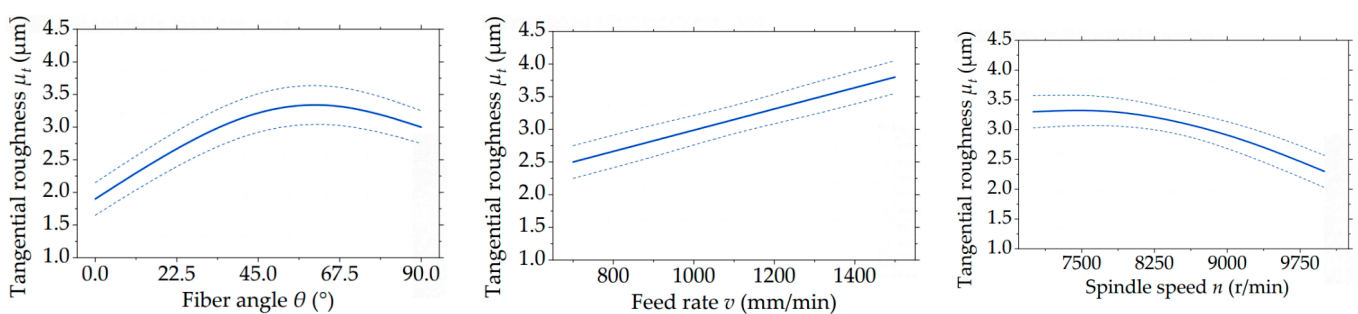


Figure 3. Relationship between tangential roughness μ_t (Ra) and the three factors (all other factors were placed at the 0 level). The dashed area represents the 95% confidence interval.

The relationship between the normal roughness μ_n and the factors is depicted in Figure 4. From the graph, it is evident that the normal roughness increased in a linear fashion as the fiber angle increased. This observation implied that the surface formed by isotically cutting ($\theta = 0^\circ$) bamboo fibers is smoother, compared to the surface formed by transversely cutting ($\theta = 90^\circ$) bamboo fibers. Furthermore, Figure 5 shows that the normal roughness exhibited a linear increase with an increase in feed rate and a decrease in spindle

speed. This finding aligned with the conclusions drawn from our previous studies on the circumferential milling performance of wood [23].

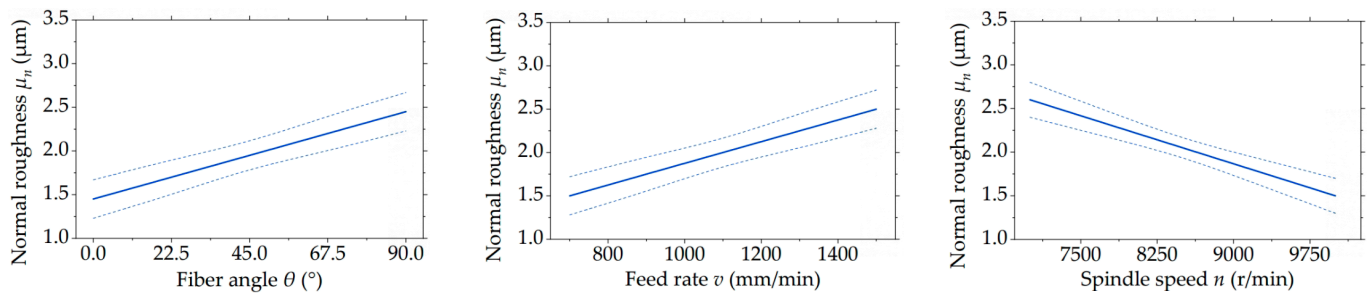


Figure 4. Relationship between normal roughness μ_n (Ra) and the three factors (all other factors were placed at the 0 level). The dashed area represents the 95% confidence interval.

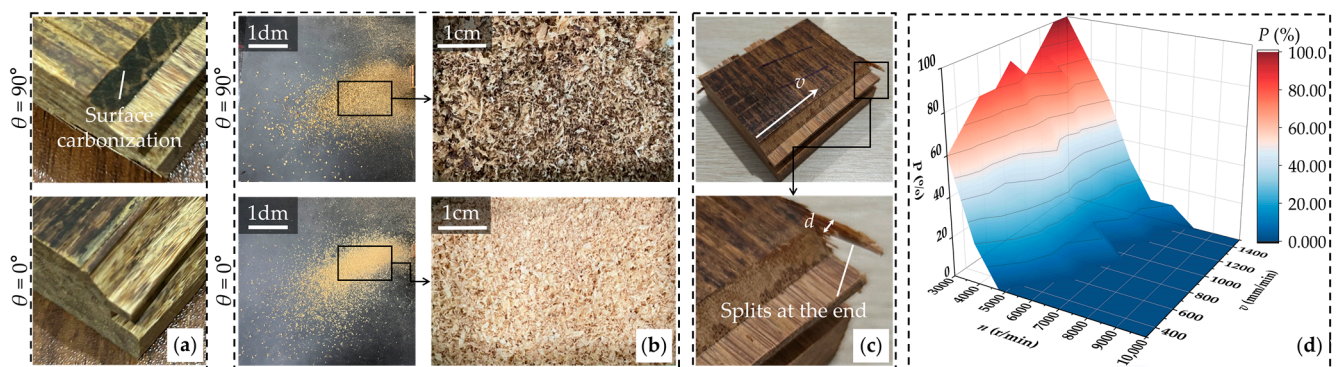


Figure 5. Defects after milling of reconstituted bamboo at low rotational speeds. (a) Carbonization of normal surface at $n = 4000$ r/min, $v = 1100$ mm/min. (b) Chips produced by milling at $n = 4000$ r/min, $v = 1100$ mm/min. (c) Splitting at the milling end, d is the width of the split. (d) Probability surface of splitting at the end, P is the probability of splitting at the end.

3.2. Analysis of Milling Surface Defects

During the milling tests of recombinant bamboo, we observed surface carbonization and end splitting as common defects, specifically occurring at $\theta = 90^\circ$. These defects negatively impact the aesthetic and ornamental properties of recombinant bamboo. To further investigate the causes of these machining defects, we conducted an extended milling test using 640 specimens with $\theta = 90^\circ$. The spindle speed n ranged from 3000 r/min to 10,000 r/min, and the feed speed v ranged from 450 mm/min to 1500 mm/min. The test results are presented in Figure 5. Additionally, each set of machining parameters was repeated ten times to calculate the probability of splitting occurrence P . The calculated probabilities are given in Table 5 and Figure 5d.

Table 5. The results of the calculation of the splitting probability P .

v (mm/min)	n (r/min)								
	3000	3875	4750	5625	6500	7375	8250	9125	10,000
300	60%	20%	0%	0%	0%	0%	0%	0%	0%
450	70%	40%	20%	0%	0%	0%	0%	0%	0%
600	80%	40%	30%	10%	0%	0%	0%	0%	0%
750	80%	50%	40%	10%	0%	0%	0%	0%	0%
900	90%	60%	50%	10%	10%	0%	0%	0%	0%
1050	80%	60%	40%	10%	0%	0%	0%	0%	0%
1200	90%	80%	40%	20%	10%	0%	0%	0%	0%
1350	100%	70%	50%	20%	10%	0%	0%	0%	0%
1500	100%	80%	60%	30%	10%	10%	0%	0%	0%

Based on the experiment that was conducted, it was discovered that surface carbonization was a significant issue for reconstituted bamboo with a fiber angle of 90° , while there were no signs of carbonization for recombinant bamboo with a fiber angle of 0° , which were milled under identical conditions. This observation led to the conclusion that surface carbonization was only related to the fiber angle of the bamboo, as evidenced by the trend shown in Figure 5a. Furthermore, the chips resulting from the milling process of the two types of bamboo displayed significant color differences, as presented in Figure 5b.

Another finding was that the end-splitting potential of the reconstituted bamboo with a fiber angle of 90° significantly increased when the spindle speed was below 6000 r/min. Notably, the splitting phenomenon predominantly occurred toward the end of the milling process, as depicted in Figure 5c,d. As expected, the generation of splitting is directly influenced by the ratio of spindle speed and feed rate, as both factors affect the direction and magnitude of cutting force. Interestingly, in practical applications, the occurrence of splitting is more dependent on the spindle speed, as demonstrated in Figure 5d. The width of cleavage d was noted to be more related to the ratio of the feeding rate and the spindle speed. Notably, an increase in the ratio of the feeding rate to the spindle speed resulted in a greater width of cleavage d , which ultimately led to more significant effects on reconstituted bamboo product. This process was similar to the effect and mechanism of splitting noted during log milling. As such, these findings highlighted the importance of considering the role of fiber angle, spindle speed, and feed rate on the final quality of the reconstituted bamboo product, and such consideration provides the foundation for further optimization of this material for use in various applications [24,25].

In order to improve our ability to effectively control the cleavage probability of recombinant bamboo, we conducted a thorough analysis by employing multivariate nonlinear regression techniques on the data presented in Table 5. Through this comprehensive analysis, we successfully derived an equation, denoted as $P(v,n)$, representing the cleavage probability (expressed in percentages), as shown in Equation (3). Subsequently, rigorous statistical evaluation revealed that the equation exhibited a remarkably high correlation with an R^2 value of 0.9849 and an adjusted R^2 value of 0.9832. This exceptional level of accuracy enabled the equation to serve as a highly reliable tool for accurately predicting the probability of end splitting in reconstituted bamboo during circumferential milling. Furthermore, we determined the root mean square error to be 3.962%, indicating the precision reliability of the equation in estimating the likelihood of splitting. These notable results signified the potential of the derived equation in facilitating effective control over end-splitting occurrence. By utilizing this equation, diligent adjustments can be made to the machining parameters, subsequently minimizing the occurrence of splitting.

$$P(v, n) = 6.082 - 17.64v + 3.652n + 16.12v^2 - 5.798vn - 0.2281n^2 - 4.696v^3 + 2.224v^2n + 0.1538vn^2 \quad (3)$$

Under the limited experimental conditions that we encountered during our investigation, our exploration of the carbonization mechanism of recombinant bamboo at $\theta = 90^\circ$ was not conducted in adequate depth. In addition, our determination of carbonization occurrence was solely reliant on visual inspection, which may have had some limitations in terms of accuracy and comprehensive understanding. Given these limitations, it would be beneficial for future researchers to delve deeper into this area by considering the microscopic model or the chemical composition of the carbonized. Such analyses could provide valuable insights into the adhesive nature of the carbonized tissue or identify the presence of bamboo fibers. This expanded information could then be utilized to optimize the binder used for recombinant bamboo, with the specific aim of minimizing carbonization on the normal cut surface at $\theta = 90^\circ$. Moreover, by focusing on enhancing the bonding strength between the binder and bamboo fibers, it may be possible to effectively reduce the likelihood of end splitting during the milling process. This multi-faceted approach would hold the potential to further enhance our understanding and control over carbonization and splitting phenomena in recombinant bamboo, leading to improved product quality and process optimization. Moreover, this article's investigation into the processability of

reorganized bamboo primarily focused on surface roughness control and prevention of splitting. However, future studies could explore other aspects of machinability, including tool wear, cutting force control, and vibration suppression.

4. Conclusions

The present study utilized an experimental methodology to examine the milling machinability of recombinant bamboo, a novel composite material. This research aimed to establish the relationship between the machining parameters for smooth milling and the tangential and normal roughness, as well as the minimum spindle speed and the minimum feed speed required to prevent surface carbonization. By analyzing these factors, we aimed to optimize the milling process and expand the applications of recombinant bamboo.

Our findings indicated that both tangential and normal roughness increase linearly with an increase in the feed rate. Furthermore, spindle speed has a profound impact on tangential roughness, leading to an accelerated decrease as the speed increases. Conversely, normal roughness decreases linearly with an increase in spindle speed. Similarly, tangential roughness initially increases, then decreases as the fiber angle increases, while normal roughness increases linearly.

Moreover, during our study, we identified that an adequate spindle speed and an appropriate feed rate are essential for preventing milling defects such as carbonization of the end face and end splitting. Overall, this study represents a preliminary exploration of refined quantitative processing of recombinant bamboo, which could facilitate quantifying the machinability of recombinant bamboo and expanding its potential applications. Areas for future research were also highlighted.

Author Contributions: Conceptualization, T.L.; methodology, Y.D.; software, T.L.; validation, Y.M.; formal analysis, T.L.; investigation, Y.C.; resources, J.Z.; data curation, C.S.; writing—original draft preparation, Y.D.; writing—review and editing, T.L.; visualization, T.L.; supervision, C.Y.; project administration, C.Y.; funding acquisition, J.Z. All authors have read and agreed to the published version of the manuscript.

Funding: This research was funded by “Major Special R&D Programs in Guangdong Province (2020B020216001)”, “The Fundamental Research Funds for the Central Universities (2572023CT14-01)” and “Key Programs of Heilongjiang Provincial Nature Fund (ZD2021E001)”.

Institutional Review Board Statement: Not applicable.

Informed Consent Statement: Not applicable.

Data Availability Statement: Not applicable.

Acknowledgments: We thank Wen Qu and Tao Zhang for fruitful discussions on xylem anatomy and technical aspects of the measurements.

Conflicts of Interest: The authors declare no conflict of interest.

References

1. Fu, Y.; Fang, H.; Dai, F. Study on the properties of the recombinant bamboo by finite element method. *Compos. Part B Eng.* **2017**, *115*, 151–159. [[CrossRef](#)]
2. Fuming, C.; Ge, W.; Cheng, H.; Li, X. Development of Advanced Bamboo Fiber Based Composites Material. *J. North-East For. Univ.* **2016**, *44*, 80–85.
3. Yu, Y.L.; Huang, X.A.; Yu, W.J. High Performance of Bamboo—Based Fiber Composites from Long Bamboo Fiber Bundles and Phenolic Resins. *J. Appl. Polym. Sci.* **2014**, *131*, 40371. [[CrossRef](#)]
4. Sharma, B.; Gatóo, A.; Bock, M.; Ramage, M. Engineered bamboo for structural applications. *Constr. Build. Mater.* **2005**, *81*, 66–73. [[CrossRef](#)]
5. Lou, L.; Fu, Y. Sound insulation performance of bamboo/polyurethane composite. *J. Text. Res.* **2017**, *38*, 73–77.
6. Huang, Y.; Ji, Y.; Yu, W. Development of bamboo scrimber: A literature review. *J. Wood Sci.* **2019**, *65*, 25. [[CrossRef](#)]
7. Zhong, Y.; Wu, G.; Ren, H.; Jiang, Z. Bending properties evaluation of newly designed reinforced bamboo scrimber composite beams. *Constr. Build. Mater.* **2017**, *143*, 61–70. [[CrossRef](#)]

8. Radzi, A.M.; Zaki, S.A.; Hassan, M.Z.; Ilyas, R.A.; Jamaludin, K.R.; Daud, M.Y.M.; Aziz, S.A. Bamboo-Fiber-Reinforced Thermoset and Thermoplastic Polymer Composites: A Review of Properties, Fabrication, and Potential Applications. *Polymers* **2022**, *14*, 1387. [[CrossRef](#)]
9. Garg, V.K.; Gaugler, R.E. Effect of coolant temperature and mass flow on film cooling of turbine blades. *Int. J. Heat Mass Transf.* **1997**, *40*, 435–445. [[CrossRef](#)]
10. Liu, W.; Yu, Y.; Hu, X.; Han, X.; Xie, P. Quasi-brittle fracture criterion of bamboo-based fiber composites in transverse direction based on boundary effect model. *Compos. Struct.* **2019**, *220*, 347–354. [[CrossRef](#)]
11. Jian, H. Forecasting model of the elasticity modulus of the aligned bamboo-wood composite panel. *J. Nanjing For. Univ. Nat. Sci. Ed.* **2009**, *33*, 33–36.
12. da Costa, L.L.; Loiola, R.L.; Monteiro, S.N. Diameter dependence of tensile strength by Weibull analysis: Part I bamboo fiber. *Materia* **2010**, *15*, 110–116. [[CrossRef](#)]
13. Liu, H.; Jiang, Z.; Sun, Z.; Yan, Y.; Cai, Z.; Zhang, X. Impact performance of two bamboo-based laminated composites. *Eur. J. Wood Prod.* **2017**, *75*, 711–718. [[CrossRef](#)]
14. Yang, X.; Yan, G.; Li, Y.; Liu, J.; Xu, Z. Research on Milling Performance of a New-type Cemented Carbide Staggered-edge End Mill for Carbon Fiber-reinforced Composite. *Rare Met. Cem. Carbides* **2015**, *43*, 67–71.
15. Chen, X.Z.; Wang, L.G.; Jin, Y.O. A DEM-PBM multiscale coupling approach for the prediction of an impact pin mill. *Powder Technol.* **2020**, *366*, 408–419. [[CrossRef](#)]
16. Wu, T.; Cheng, K. An investigation on the cutting performance of nano-crystalline diamond coatings on a micro-end mill. *Proc. Inst. Mech. Eng. Part B J. Eng. Manuf.* **2012**, *226*, 1421–1424. [[CrossRef](#)]
17. Zhao, Z.; Liu, X.; Yue, C.; Li, R.; Zhang, H.; Liang, S. Tool Quality Life during Ball End Milling of Titanium Alloy Based on Tool Wear and Surface Roughness Models. *Appl. Sci.* **2020**, *10*, 3316. [[CrossRef](#)]
18. Yang, Y.; Yang, Y.; Li, Q.; Qin, Y.; Yang, G.; Zhou, B.; Deng, C.; Wu, M. An eco-friendly pulsed magnetic field treatment on cemented carbide (WC-12Co) for enhanced milling performance. *J. Clean. Prod.* **2022**, *340*, 130748. [[CrossRef](#)]
19. Tian, X.C.; Yu, W.J.; Ma, H.X. Changing law and prediction model of temperature field during the preparation of recombinant bamboo. *J. For. Eng.* **2023**, *8*, 38–45. (In Chinese)
20. Vilotic, D.; Alexandrov, S.; Ivanisevic, A.; Milutinovic, M. Reducibility of Stress-Based Workability Diagram to Strain-Based Workability Diagram. *Int. J. Appl. Mech.* **2016**, *8*, 1650022. [[CrossRef](#)]
21. Liu, J.; Cui, Z.S.; Li, C.X. Analysis of metal workability by integration of FEM and 3-D processing maps. *J. Mater. Process. Technol.* **2008**, *205*, 497–505. [[CrossRef](#)]
22. Obour, P.B.; Lamandé, M.; Edwards, G.; Sørensen, C.G.; Munkholm, L.J. Predicting soil workability and fragmentation in tillage: A review. *Soil Use Manag.* **2017**, *33*, 288–298. [[CrossRef](#)]
23. Yang, C.; Liu, T.; Ma, Y.; Qu, W.; Ding, Y.; Zhang, T.; Song, W. Study of the Movement of Chips during Pine Wood Milling. *Forests* **2023**, *14*, 849. [[CrossRef](#)]
24. Ostapska, K.; Malo, K.A. Crack path tracking using DIC and XFEM modelling of mixed-mode fracture in wood. *Theor. Appl. Fract. Mech.* **2021**, *112*, 102896. [[CrossRef](#)]
25. Wargula, L.; Wojtkowiak, D.; Kukla, M.; Talaska, K. Modelling the process of splitting wood and chipless cutting *Pinus sylvestris* L. wood in terms of designing the geometry of the tools and the driving force of the machine. *Eur. J. Wood Wood Prod.* **2022**, *81*, 223–237. [[CrossRef](#)]

Disclaimer/Publisher’s Note: The statements, opinions and data contained in all publications are solely those of the individual author(s) and contributor(s) and not of MDPI and/or the editor(s). MDPI and/or the editor(s) disclaim responsibility for any injury to people or property resulting from any ideas, methods, instructions or products referred to in the content.